Desalination and Water Treatment
www.deswater.com

doi: 10.1080/19443994.2014.932714

56 (2015) 223–231
September

Taylor & Francis
Taylor & Francis Group

Adsorption of Pb(II) from aqueous solutions using corn straw

Dongmei Jia[a,b,*], Changhai Li[a,b,*]

[a] *Engineering Research Center for Wastewater Resource of Shandong Province, Binzhou 256603, China, Tel. +86 05433169538; Fax: +86 05433169538; emails: jiadm2005@163.com (D. Jia), lichanghai@bzu.edu.cn (C. Li)*
[b] *Department of Chemical Engineering, Binzhou University, Binzhou 256603, China*

Received 17 January 2014; Accepted 1 June 2014

ABSTRACT

Large amounts of wastewater containing heavy metals are discharged from electroplating, metal finishing, textile, and other industrial plants, bringing health risks to humans and animals. There is, therefore, a growing concern to find low cost and effective ways to remove heavy metals from wastewater. In the present study, untreated corn straw was used as an adsorbent, and basic parameters for lead Pb(II) adsorption were studied. The Pb(II) adsorption was found to be dependent on contact time, pH, adsorbent dosage, initial concentration of Pb(II), and temperature. The kinetics were studied using pseudo-first order, pseudo-second order, Elovich, and Weber–Morris models, and the kinetic parameters were determined. The untreated corn straw particles showed the maximum adsorption capacity (15.0269 mg/g) for Pb(II). The adsorption isotherms indicated that the heat of adsorption linearly increased as the thickness of the Pb(II) layer on the adsorbent gradually increased. The studies showed that corn straw can be used as a good adsorbent material for Pb(II) removal from aqueous solutions.

Keywords: Pb(II); Corn straw; Adsorption; Kinetics; Isotherms

1. Introduction

Water contamination by heavy metals is a serious threat to the global ecosystem. Adsorption, ion exchange, coagulation, floatation, hyper-filtration, chemical precipitation, and reverse osmosis are usually used for removing heavy metals from aqueous solutions [1]. Low cost, effective, and environmental friendly methods need to be developed, that can be easily implemented to clean lead or other toxic metals from contaminated areas and industrial wastewaters [2]. Adsorption has proven to be the most efficient method for quickly lowering the concentration of heavy metals in aqueous solutions [3]. Currently, there is much interest in developing bioadsorbents because of their high versatility, metal selectivity, high uptake, concentration independence, and high tolerance for organics and regeneration [4]. Researchers are presently oriented towards low-cost materials such as rice husks, fly ash, pine bark, sawdust, animal bones, walnut shells, tree bark, lignin, chitin, chitosan, and peat moss for removal of heavy metal ions [5]. Corn straw (CS) is an agricultural by-product, and its major advantages include low cost, and that it is associated with minimal chemical or biological sludge, adsorbent regeneration, and the possibility of effluent recovery. In this regard, studies have been carried out to investigate the potential of CS adsorption for the removal of lead from aqueous solutions by collection and analysis

---

*Corresponding authors.

of adsorption data. The pH, adsorbent dosage, contact time, and temperature in the adsorption process were measured to provide more information about the adsorption characteristics of CS. The surface and pore structure of CS were then characterized based on nitrogen adsorption isotherms and Fourier transform infrared (FTIR) analysis.

2. Experiment

2.1. Preparation and characterization of the adsorbent

The adsorbent used in this study was waste CS from cafeterias. The CS was crushed and separated from its chaff, and sieved to mesh ranges of 100–150 mesh, washed with distilled water, and then dried at 50˚C for at least 10 h.

The surface area, pore volume, and pore size of the adsorbent were determined by N_2 adsorption using a TriStar II 3010 Surface Area & Pore Size Analyzer (Micromeritics Instrument, USA). The Brunauer–Emmett–Teller (BET) surface area was obtained by applying the BET equation to the adsorption data. The pore size distribution was obtained using the Barrett–Joyner–Halenda (BJH) method. FTIR spectra of the CS were recorded as KBr pellets (1 mg CS in 100 mg of KBr) from 400 to 4,000 cm^{-1} on a NICOLET-380 FTIR (Thermo Fischer Scientific, Waltham, Massachusetts). Morphological analysis of the CS was performed using field emission scanning electron microscopy (SEM), (Sirion 200 FEI, Hillsboro, OR).

2.2. Preparation of the metal solution

Divalent Pb(II) solutions were prepared by dissolving lead nitrate ($Pb(NO_3)_2{\cdot}4H_2O$) in distilled water. The initial concentrations varied from 10 to 60 mg/L. The pH of the solution was adjusted using a solution of HNO_3 or NaOH.

2.3. Pb(II) adsorption experiments

The adsorption experiments were carried out in batch mode at room temperature. A given mass of adsorbent was added to the lead solution, and the resulting sample was agitated for a prescribed amount of time. The samples were then filtered through filter paper at discrete time intervals. To calculate the rate of lead adsorption (*Re*), we used the following expression [6]:

$$Re\,(\%) = \frac{C_0 - C_e}{C_0} \times 100\% \tag{1}$$

where C_0 and C_e are the initial and residual concentrations (mg/L) of Pb(II) in solution, respectively.

2.4. Adsorption kinetics

A kinetics study of adsorption is necessary, as it provides information on the adsorption mechanism, which is crucial for the practicality of the process. Four rate equations have been applied to correlate the kinetic data of adsorption to different controlling steps in the adsorption process.

The pseudo-first-order kinetic model is frequently used in kinetic studies [7]. It is expressed by the following equation:

$$\log(q_e - q_t) = \log(q_e) - \frac{k_1}{2.303}t \tag{2}$$

where k_1 (1/h) is the rate constant of pseudo-first-order adsorption, which is obtained from the slopes of the linear plots of $\log(q_e - q_t)$ vs. t.

The pseudo-second-order kinetic model may be expressed by the equation [8]:

$$\frac{t}{q_t} = \frac{1}{k_2 q_e^2} + \frac{t}{q_e} \tag{3}$$

where k_2 (g/(mg h)) is the equilibrium rate constant for the pseudo-second-order adsorption, and can be obtained from the plot of t/q_t against t.

The Elovich model describes a number of reaction mechanisms, including bulk and surface diffusion and the activation and deactivation of catalytic surfaces [9]. It is represented as:

$$q_t = a + b \ln t \tag{4}$$

where a (mg/g) and b (mg/(g min)) are the constants of the adsorption, and are determined from the plot of q_t vs. $\ln t$.

The Weber–Morris model is defined by the following equation [10]:

$$q_t = k_t t^{0.5} + c \tag{5}$$

where k_t (g/mg $h^{1/2}$) is the constant of the adsorption, and is determined from the plot of q_t vs. $t^{0.5}$.

2.5. Adsorption isotherms

The Langmuir model is generally expressed as follows [11]:

$$q_e = \frac{q_{\max} K_L C_e}{1 + K_L C_e} \tag{6}$$

where C_e (mg/L) is the equilibrium concentration of Pb(II) in a solution, K_L (L/mg) is the Langmuir constant, which is related to the affinity of binding sites, and $q_{\max}$ (mg/g) is the monolayer adsorption capacity.

The Freundlich isotherm is expressed as follows [12]:

$$q_e = K_F C_e^{\frac{1}{n}} \tag{7}$$

where K_F (L/mg) and n are Freundlich constants, which represent adsorption capacity and adsorption strength, respectively.

The Redlich–Peterson isotherm [13] can be described as follows:

$$q_e = \frac{K_R C_e}{1 + b_R C_e^m} \tag{8}$$

It has three isotherm constants, namely, K_R (L/mg), b_R $(\mathrm{L/mg})^m$, and m. K_R and b_R are the adsorption constants related to the energy of adsorption and binding forces between adsorbate and adsorbent, respectively.

The Temkin isotherm can be used to study the heat of adsorption and adsorbate-adsorbent interaction on the adsorbent surface [14]. Eq. (9) shows the linear form of this isotherm:

$$q_e = B_1 \ln K_T + B_1 \ln C_e \tag{9}$$

where B_1 is the Temkin adsorption constant, and K_T (mg/L) is the equilibrium binding constant. K_T is the equilibrium binding constant corresponding to the maximum binding energy, whereas B_1 is related to the heat of adsorption [15].

3. Results and discussion

3.1. Characterization of the adsorbent

Some characteristics of CS are presented in Table 1. To gain insight to the structural properties of the adsorbent, it was characterized by BET, SEM, and FTIR. SEM micrographs of the CS are shown in Fig. 1(a) and (b). Regular and porous surfaces can be observed in the micrographs. A rough surface and abundant pores would provide convenient diffusion channels for ions onto the CS. Therefore, it can be concluded that CS presents an adequate morphology for metal adsorption. Fig. 2 shows the infrared spectra of the CS and the CS loaded Pb(II); the loaded Pb(II) induced some minor modifications of the infrared spectra. The broad band from 1,000 to 1,200 cm^{-1} can be attributed to the cellulose, indicating that the skeleton of CS is a cellulose chain. The band at 1,054 cm^{-1} can be assigned to aliphatic ether (C–O) stretching [16]. The peak observed at 3,423 cm^{-1} can be attributed to the stretching of O–H groups due to inter- and intra-molecular hydrogen bonding of compounds. The band at 2,917 cm^{-1} indicates symmetric or asymmetric C–H stretching vibration of aliphatic acids. The band at 1,630 cm^{-1} represents the contribution from aromatic C=O stretching. The presence of a weak absorption peak at 1,382 cm^{-1} is confidently attributed to the C–O stretching of carboxylate anions. On the infrared spectra of CS loaded Pb(II), the peak at 1,373 cm^{-1} likely indicates the interactions between carboxylate anions ($-\mathrm{COO}^-$) and Pb(II) [17].

3.2. Effect of adsorbent dosage and concentration

Fig. 3 shows the effect of adsorbent dosage on the Pb(II) removal efficiency for a constant Pb(II) concentration (20 mg/L) at 298 K. The Pb(II) removal efficiency increased rapidly from 44.50 to 90.75% with increasing adsorbent dosage from 0.05 to 0.2 g, and then decreased gradually to 78.16% with further increase in adsorbent dosage. The maximum removal efficiency was 90.75%. The increase in adsorbent dosage did not obviously give rise to Pb(II) removal efficiency. This was due to active adsorption sites being occupied, but not remaining saturated. Accordingly, the increase in adsorbent dosage did not provide higher uptake of Pb(II) ions.

When the concentration of Pb(II) was increased and the amount of adsorbent held constant (0.2 g), the adsorption decreased for the same adsorption time (Fig. 4). The adsorption decreased from 90.75 to 75.40% as the Pb(II) concentration was increased from 20 to 60 mg/L for a CS amount of 0.2 g. The lower uptake at higher concentration can be explained as the total number of available adsorption sites being fixed for a given adsorbent dose, hence adsorbing almost the same amount of adsorbate, thus resulting in a decrease in the removal of adsorbate, corresponding to an increase in initial adsorbate concentration.

Table 1
Characterization of CS

Surface area (m^2/g)			Pore volume (mL/g)		Pore size (nm)	
BET	Single point	BJH adsorption	Single point	BJH adsorption	BET	BJH adsorption
21.008	16.686	4.415	0.0173	0.00252	3.294	2.288

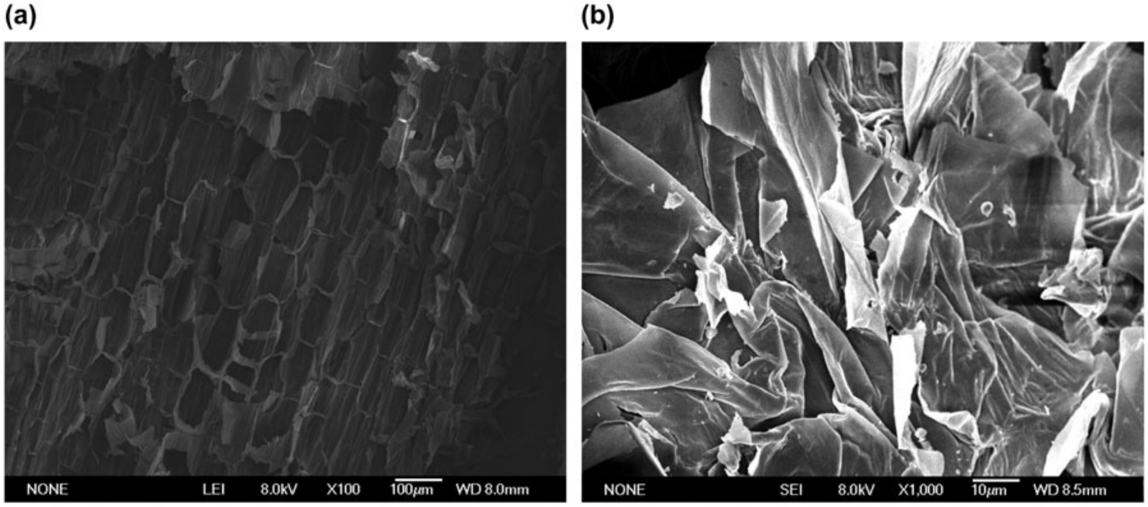

Fig. 1. SEM micrographs of CS.

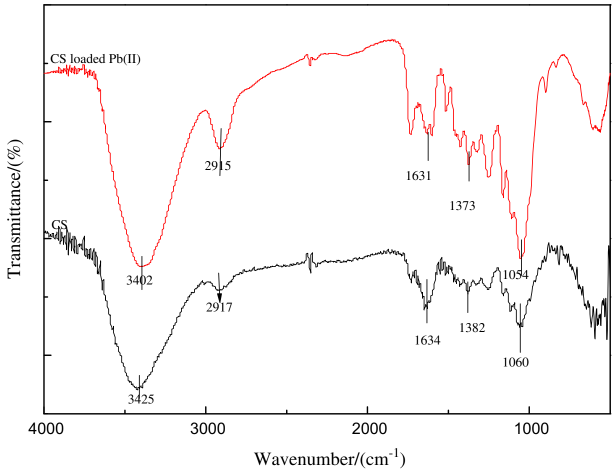

Fig. 2. FTIR spectrum of CS and Cs loaded Pb(II).

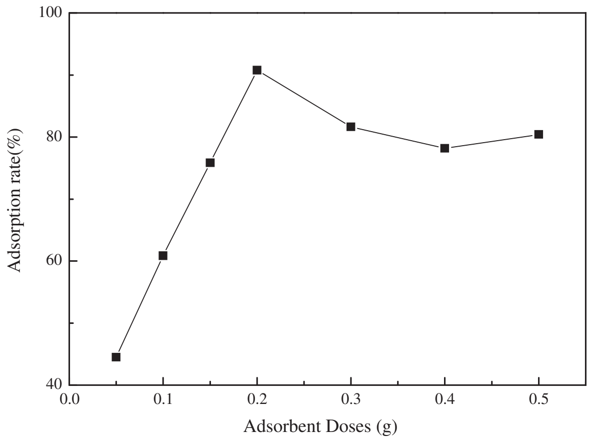

Fig. 3. Effect of adsorbent dosage on Pb(II) removal efficiency by CS.

3.3. Effect of pH on the removal of Pb(II)

Fig. 5 shows the variation of Pb(II) removal efficiency with initial pH of the solution. It is clear that the pH of the solution has a significant impact on the adsorption of Pb(II) onto CS. A slight increase in adsorption was found as the pH was increased from 2 to 4, while a more significant decrease was obtained at a pH of 5, and then flattened to reach a maximum at 92.06% with a further increase in pH to 6. At pH < 6.5, the dominant species of Pb(II) is Pb^{2+} and $Pb(OH)^{+}$

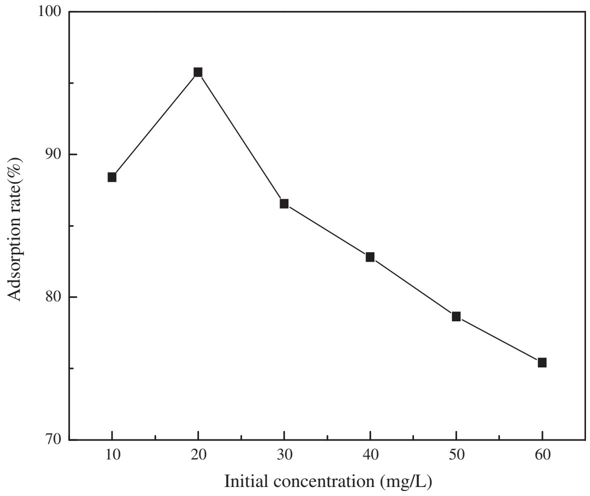

Fig. 4. Effect of initial concentration on Pb(II) removal efficiency by CS.

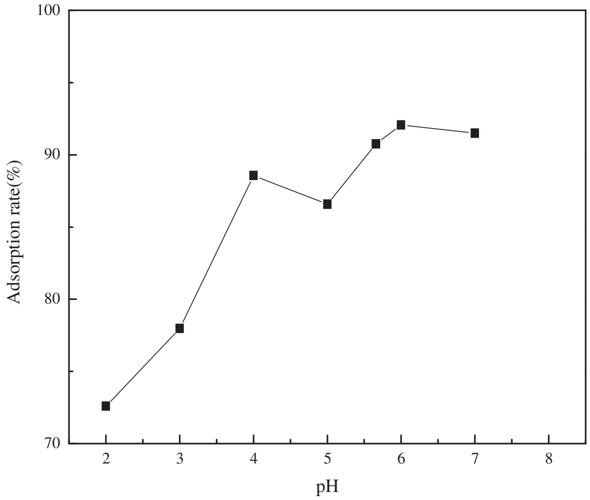

Fig. 5. Effect of pH on Pb(II) removal efficiency by CS.

[18]. The Pb(II) adsorption on the CS may be caused by large amounts of relatively easily accessible hydroxyl and carboxyl groups in the CS [19], as the result of FTIR analysis (Fig. 2) proved that hydroxyl and carboxyl groups are present in CS particles. Therefore, it is believed that the adsorption of Pb(II) on CS is dominated by electrostatic attraction depending on the functional groups –COO^- and Pb^{2+} [20]. This may be due to active adsorption sites remaining protonated at low pH, and becoming less available for metal ion adsorption [21]. As pH increases, the concentration of H^+ ions decreases, hence they do not compete with metal ions on the adsorption sites. This variation is quite similar to previous reports [22,23]. Several studies have been conducted using various adsorbents for Pb(II) removal. Table 2 presents a comparison of the optimum pH of various adsorbents for Pb(II) adsorption. It can be seen from Table 2 that the optimum pH of CS to Pb(II) adsorption is within the range of other studies.

3.4. Effect of time and kinetics

The kinetics were investigated with constant amounts of CS at 298 K with four different Pb(II) concentrations, 10, 20, 30, and 40 mg/L, for interaction time intervals of 20 min. Fig. 6 indicates that most of the adsorption process takes place during the late stages. Such behavior is expected in a batch reaction with either a constant adsorbent amount or varying initial adsorbate concentration, or vice versa [34]. In the present case, the adsorbate-adsorbent interactions approached equilibrium after approximately 3 h. The kinetic rate constants and correlation coefficient values (R^2) obtained from pseudo-first order, pseudo-second order, Elovich, and Weber–Morris models are given in Table 3. It is clear that the pseudo-second-order kinetics possess higher correlation coefficient values (0.99–1) than the other models. The predominant process of Pb(II) adsorption onto CS may be chemisorption, which is usually restricted to just one layer of molecules on the surface, although it may be followed by additional layers of physically adsorbed molecules [35]. The mechanism of adsorption commonly involves three steps: (a) the Pb(II) is transferred across the external boundary layer film of liquid surrounding the outside of the particle; (b) the Pb(II) is diffused to the adsorption site; and (c) the Pb(II) is adsorbed at sites on the surface. For Pb(II) adsorption onto CS, we attempted to predict the mechanism of adsorption and desorption as shown in Fig. 7. The adsorption of Pb (II) may explained as the surface active sites being all occupied, and the adsorbates diffusing into the inner pores for further interaction.

3.5. Adsorption isotherm

The adsorption isotherm results (Fig. 8) and constants of the Langmuir, Freundlich, Redlich–Peterson, and Temkin isotherm models are given in Table 4. The result of regression analysis to calculate the parameters of four isotherms indicated that the value of maximum adsorption capacity per unit weight of adsorbent for the Langmuir model is 15.0269 mg/g. The values of n and K_F obtained from the Freundlich model were 0.4975 and 3.0364 L/g, respectively. Table 4 shows that the Freundlich model had the

Table 2
The optimum pH of various adsorbent to Pb(II) adsorption

Adsorbent	Optimum or used pH	References
Goethite	5.5	[24]
Red pozzolan	6.0	[25]
Activated carbon surface modifications	5.5	[26]
Basic oxygen furnace slag	6.0	[27]
Azadirachta indica (Neem) leaf powder	7.0	[1]
Sea nodule residues	5.6	[28]
Poly(ethylene terephthalate)-g-acrylamide fibers	5.5	[29]
Bamboo dust carbon	7.2	[30]
Commercial activated carbon	7.2	
Peanut hull ash	6.0	[31]
Leaves of date trees	5.8	[32]
Pine cone activated carbon	6.7	[33]
Portulaca plant	6.0	[22]
Corn straw	6.0	Present study

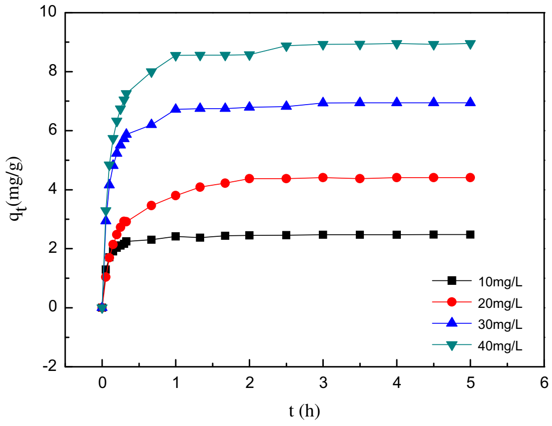

Fig. 6. Effect of time on adsorption of Pb(II) onto CS.

lowest values of regression coefficients compared to the other isotherm models. The results show that the Temkin model was the more favorable model, and the heat of adsorption linearly increased as the thickness of the Pb(II) layer on the adsorbent gradually increased, because of reduced adsorbate-adsorbent interaction [36].

The essential characteristic of the Langmuir equation can be expressed in terms of a dimensionless separation factor R_L, which is defined as:

$$R_L = \frac{1}{1 + K_L C_0} \tag{10}$$

where C_0 is the initial dye concentration and R_L indicates the nature of the adsorption process. The calculated R_L values indicated adsorption of Pb(II) on CS was favorable.

Table 3
Values of kinetic model parameters estimated for the Pb(II) adsorption on CS

Kinetic models	Parameters	10 mg/L	20 mg/L	30 mg/L	40 mg/L
Pseudo-first-order model	k_1 (h^{-1})	1.5440	1.5871	1.6461	1.5452
	R^2	0.9403	0.8516	0.9533	0.9456
Pseudo-second-order model	k_2 (g/(mg h))	0.000875	0.006403	0.000692	0.000858
	R^2	1.0000	0.9994	0.9999	0.9999
Elovich model	a (mg/g)	0.3631	0.9302	1.2166	1.743
	b (mg/(g min))	1.0537	0.1009	2.0044	1.7835
	R^2	0.9206	0.9889	0.9511	0.9725
Weber–Morris model	k_t (g/(mg min)$^{1/2}$)	0.1599	0.4301	0.5455	0.7910
	c (mg/g)	1.3573	0.7935	2.9809	3.1433
	R^2	0.7537	0.8927	0.8704	0.8457

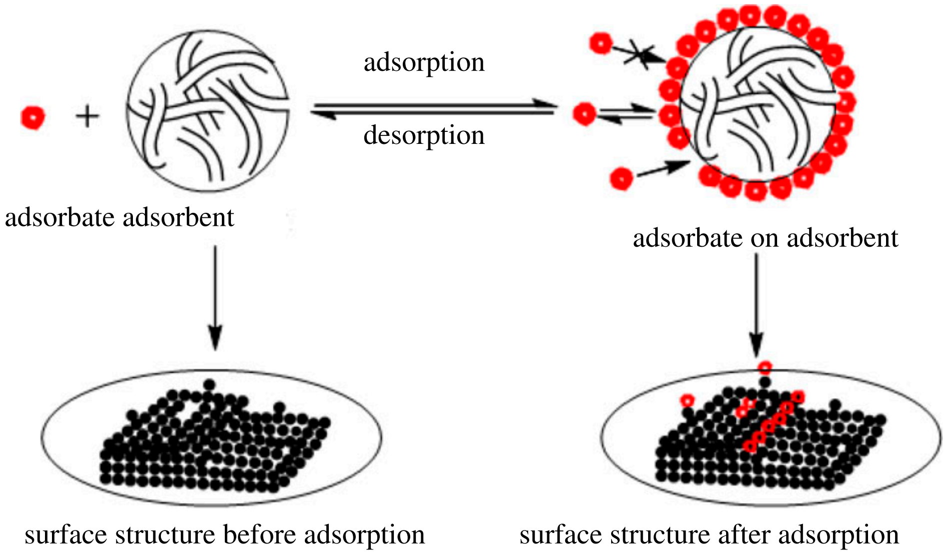

Fig. 7. The adsorption and desorption mechanism of Pb(II) onto CS.

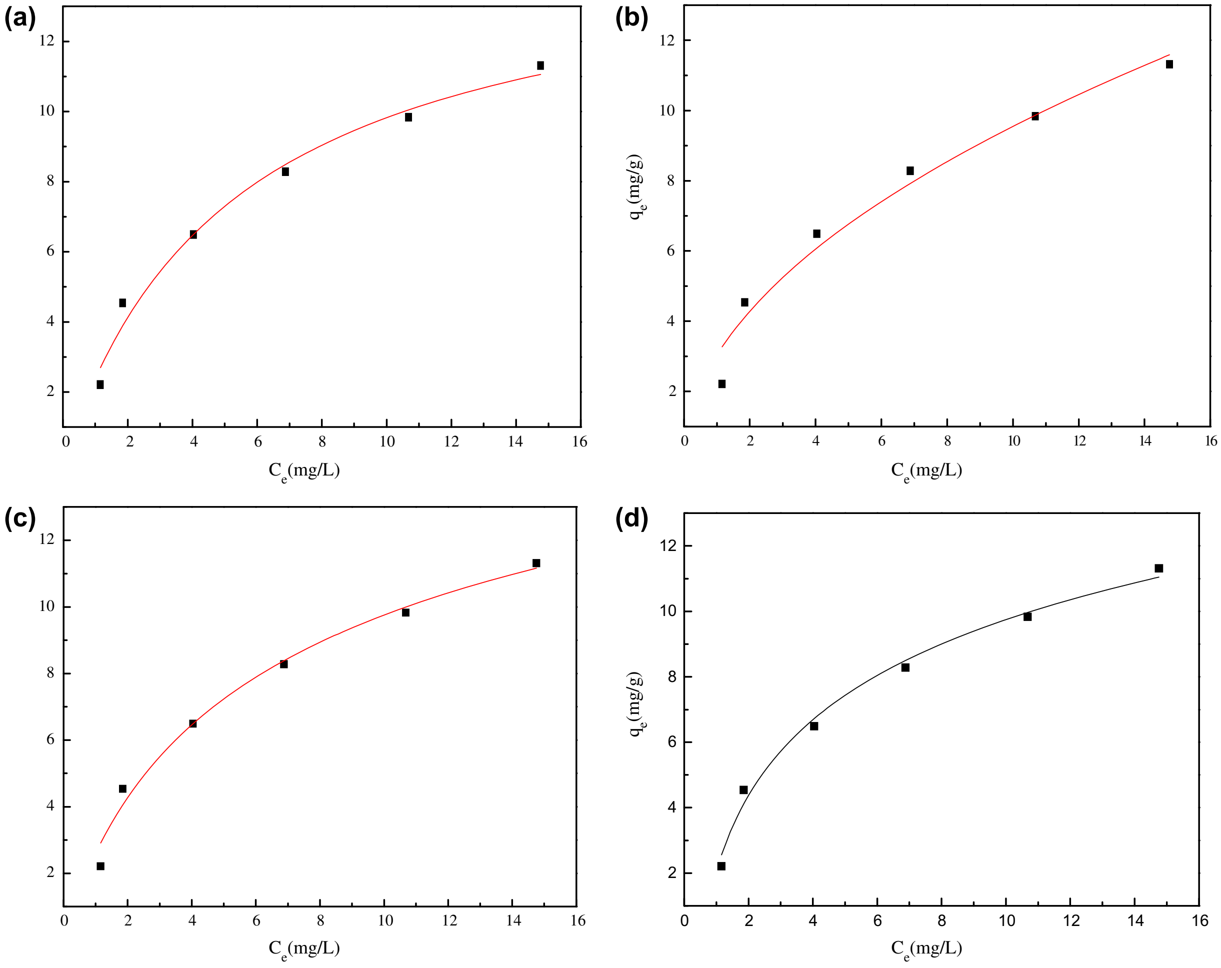

Fig. 8. Isotherm models of (a) Langmuir, (b) Freundlich, (c) Redlich–Peterson, and (d) Temkin for adsorption of Pb(II) onto CS.

Table 4
Equilibrium model parameters for adsorption of Pb(II) onto CS

Equilibrium model	Parameter	Value
Langmuir isotherm	K_L (L/mg)	0.03226
	$q_{\max}$ (mg/g)	15.0269
	R^2	0.9823
	R_L	0.3406–0.7560
Freundlich isotherm	K_F (L/g)	3.0364
	n	0.4975
	R^2	0.9638
Redlich–Peterson isotherm	K_R (L/g)	3.2506
	b_R (L/mg)$^{\mathrm{m}}$	0.3005
	m	0.8896
	R^2	0.9781
Temkin isotherm	K_T (L/mg)	1.7799
	B_1	3.3834
	R^2	0.9898

4. Conclusion

CS was used as an adsorbent for removal of Pb(II) from aqueous solutions. This material exhibited outstanding adsorption performance for Pb(II) with a removal efficiency of 90.75%. The optimal parameters for the adsorption process were: an adsorbent dose of 0.2 g, a pH of 6, and a temperature of 298 K. The kinetic experiments showed that the adsorption was rapid, and maximum adsorption capacities were achieved in 3 h. The adsorption process was well fit by the pseudo-second-order model, and the adsorption equilibrium followed the Langmuir model, which gave the maximum adsorption capacity of 15.0269 mg/g at 298 K. The results indicate that CS may be effectively used as an adsorbent without any treatment for the removal of lead from aqueous solutions.

Acknowledgments

This research was funded by the Shandong Provincial Natural Science Foundation, China (Grant No. ZR2013EML001) and the Binzhou University Natural Science Foundation, China (Grant No. 2012ZDL03 and 2013Y02).

References

[1] K.G. Bhattacharyya, A. Sharma, Adsorption of Pb(II) from aqueous solution by *Azadirachta indica* (neem) leaf powder, J. Hazard. Mater. 113 (2004) 97–109.

[2] M.I. Khalil, S. Farag, Utilization of some starch derivatives in heavy metal ions removal, J. App. Poly. Sci. 69 (1998) 45–50.

[3] Z.Z. Li, X.W. Tang, Y.M. Chen, L.M. Wei, Y. Wang, Activation of *Firmiana Simplex* leaf and the enhanced Pb(II) adsorption performance: Equilibrium and kinetic studies, J. Hazard. Mater. 169 (2009) 386–394.

[4] B. Volesky, Biosorption of Heavy Metals, CRC Press, Boca Raton, FL, 1990.

[5] M.H. Entezari, T. Soltani, Simultaneous removal of copper and lead ions from a binary solution by sonosorption process, J. Hazard. Mater. 160 (2008) 88–93.

[6] D.M. Jia, Y.J. Li, X.L. Shang, C.H. Li, Iron-impregnated weakly basic resin for the removal of 2-naphthalenesulfonic acid from aqueous solution, J. Chem. Eng. Data 56 (2011) 3881–3889.

[7] S. Lagergren, About theory of so-called adsorption of soluble substances, K. Sven. Vetenskapsakad. Andl. 24 (1898) 1–39.

[8] Y.S. Ho, G. McKay, Pseudo-second order model for sorption processes, Process Biochem. 34 (1999) 451–465.

[9] W.J. Weber, J.C. Morris, Advances in water pollution research: Removal of biologically resistant pollutants from waste waters by adsorption, in: Proceedings of International Conference on Water Pollution Symposium, vol. 2, 1962, pp. 231–266.

[10] K. Urano, H. Tachikawa, Process development for removal and recovery of phosphorus from wastewater by a new adsorbent. II: Adsorption rates and breakthrough curves, Ind. Eng. Chem. Res. 30 (1991) 1897–1899.

[11] I. Langmuir, The constitution and fundamental properties of solids and liquids. Part I: Solids, J. Am. Chem. Soc. 38 (1916) 2221–2295.

[12] H.M.F. Freundlich, Uber die adsorption in losungen (Concerning adsorption in solutions), Z. Phys. Chem. 57 (1906) 385–470.

[13] O. Redlich, D.L. Peterson, A useful adsorption isotherm, J. Phys. Chem. 63 (1959) 1024.

[14] H.M.H. Gad, A.A. El-Sayed, Activated carbon from agricultural by-products for the removal of Rhodamine-B from aqueous solution, J. Hazard. Mater. 168 (2009) 1070–1081.

[15] I.D. Mall, V.C. Srivastava, N.K. Agarwal, I.M. Mishra, Removal of congo red from aqueous solution by bagasse fly ash and activated carbon: Kinetic study and equilibrium isotherm analyses, Chemosphere 61 (2005) 492–501.

[16] Y. Qiu, H. Cheng, C. Xu, G.D. Sheng, Surface characteristics of crop-residue-derived black carbon and lead(II) adsorption, Water Res. 42 (2008) 567–574.

[17] X.S. Wang, Z.P. Lu, H.H. Miao, W. He, H.L. Shen, Kinetics of Pb(II) adsorption on black carbon derived from wheat residue, Biochem. Eng. J. 166 (2011) 986–993.

[18] T.K. Naiya, A.K. Bhattacharya, S.K. Das, Adsorption of Pb(II) by sawdust and neem bark from aqueous solutions, Environ. Prog. 27 (2008) 313–328.

[19] T.A. Sibel, G. Asli, A. Burcu, K. Zerrin, A. Tamer, Investigation of the biosorption characteristics of lead(II) ions onto *Symphoricarpus albua*: Batch and dynamic flow studies, J. Hazard. Mater. 165 (2009) 26–133.

[20] J. Li, S. Chen, G. Sheng, J. Hu, X. Tan, X. Wang, Effect of surfactants on Pb(II) adsorption from aqueous solutions using oxidized multiwall carbon nanotubes, Chem. Eng. J. 166 (2011) 551–558.

[21] A. Hammaini, F. González, A. Ballester, M.L. Blázquez, J.A. Muñoz, Biosorption of heavy metals by activated sludge and their desorption characteristics, J. Environ. Manage. 84(4) (2007) 419–426.

[22] A. Dubey, S. Shiwani, Adsorption of lead using a new green material obtained from *Portulaca* plant, Int. J. Environ. Sci. Technol. 9 (2012) 15–20.

[23] H.H. Tran, F.A. Roddick, J.A. O'Donnell, Comparison of chromatography and desiccant silica gels for the adsorption of metal ions-I. Adsorption and kinetics, Water Res. 33 (1999) 2992–3000.

[24] D.P. Rodda, B.B. Johnson, J.D. Wells, Modeling the effect of temperature on adsorption of lead(II) and zinc(II) onto goethite at constant pH, J. Colloid Interface Sci. 184 (1996) 365–377.

[25] M.P. Papini, Y.D. Kahie, B. Troia, M. Majone, Adsorption of lead at variable ph onto a natural porous medium: Modeling of batch and column experiments, Environ. Sci. Technol. 33 (1999) 4457–4464.

[26] J. Rivera-Utrilla, I. Bautista-Toledo, M.A. Ferro-Garca, C. Moreno-Castilla, Activated carbon surface modifications by adsorption of bacteria and their effect on aqueous lead adsorption, J. Chem. Technol. Biotechnol. 76 (2001) 1209–1215.

[27] Y.J. Xue, H.B. Hou, S.J. Zhu, Competitive adsorption of copper(II), cadmium(II), lead(II) and zinc(II) onto basic oxygen furnace slag, J. Hazard. Mater. 162 (2009) 391–401.

[28] A. Agrawal, K.K. Sahu, B.D. Pandey, Systematic studies on adsorption of lead on sea nodule residues, J. Colloid Interface Sci. 281 (2005) 291–298.

[29] R. Coskun, C. Soykan, Lead(II) adsorption from aqueous solution by poly(ethylene terephthalate)-g-acrylamide fibers, J. Polym. Res. 13 (2006) 1–8.

[30] N. Kannan, T. Veemaraj, Removal of lead(II) ions by adsorption onto bamboo dust and commercial activated carbons—A comparative study, Eur. J. Chem. 6 (2009) 247–256.

[31] S.W. Liao, C.I. Lin, L.H. Wang, Kinetic study on lead (II) ion removal by adsorption onto peanut hull ash, J. Taiwan. Inst. Chem. Eng. 42 (2011) 166–172.

[32] F. Boudrahem, F. Aissani-Benissad, A. Soualah, Adsorption of lead(II) from aqueous solution by using leaves of date trees as an adsorbent, J. Chem. Eng. Data. 56 (2011) 1804.

[33] M. Milan, P. Milovan, B. Aleksandar, Z. Aleksandra, R. Marjan, Removal of lead(II) ions from aqueous solutions by adsorption onto pine cone activated carbon, Desalination 276 (2011) 53–59.

[34] M.J. Ahmed, S.K. Dhedan, Equilibrium isotherms and kinetics modeling of methylene blue adsorption on agricultural wastes-based activated carbons, Fluid Phase Equilib. 317 (2012) 9–14.

[35] E.N. El Qada, S.J. Allen, G.M. Walker, Adsorption of methylene blue onto activated carbon produced from steam activated bituminous coal: A study of equilibrium adsorption isotherm, Chem. Eng. J. 124 (2006) 103–110.

[36] Y.C. Sharma, Uma, S.N. Upadhyay, Removal of a cationic dye from wastewaters by adsorption on activated carbon developed from coconut coir, Energy. Fuels. 23 (2009) 2983–2988.